Neurochemistry International 129 (2019) 104502

Contents lists available at ScienceDirect

Neurochemistry International

journal homepage: www.elsevier.com/locate/neuint

Age-related neurochemical and behavioural changes in D409V/WT *GBA1* mouse: Relevance to lewy body dementia

E. Clarke[a,*], C. Jantrachotechatchawan[a], Y. Buhidma[a], M. Broadstock[a], L. Yu[a], D. Howlett[a], D. Aarsland[b], C. Ballard[c], P.T. Francis[a,c]

[a] King's College London, Wolfson Centre for Age-Related Diseases, UK
[b] King's College London, Department of Old Age Psychiatry, UK
[c] University of Exeter, UK

ARTICLE INFO

Keywords:
Lewy body dementia
Glucocerebrosidase
Cognitive impairment
Glia
Cholinergic integrity
Hippocampus

ABSTRACT

Heterozygous mutations in *GBA1*, the gene which encodes the lysosomal enzyme glucocerebrosidase (GCase), are a strong genetic risk factor for the development of Lewy body dementia (LBD). Until this point however, recapitulation of the symptoms and pathology of LBD has been limited to a homozygous *GBA1* mouse model which genetically and enzymatically reflects the lysosomal storage disorder Gaucher's disease.

This study reports for the first time cognitive impairment by two independent behavioural tests in heterozygous *GBA1* mutant mice (D409V/WT) which demonstrate significant cognitive impairment by the age of 12 months. Furthermore, reductions in *GBA1* GCase enzyme activity within the brain reflects levels seen in sporadic and *GBA1* mutant LBD patients. While there is no overt deposition of Lewy bodies within the hippocampus, alterations to cholinergic machinery and glial proliferation are evident, both pathological features of LBD. Interestingly, we also describe the novel finding of significantly reduced *GBA2* GCase enzyme activity specifically within the hippocampus. This suggests that reduced *GBA1* GCase enzyme activity dis-equilibrates the finely balanced glycosphingolipid metabolism pathway and that reductions in *GBA2* GCase enzyme could contribute to the pathological and behavioural effects seen.

Overall, this study presents evidence to suggest that pathological hallmarks associated with LBD specifically affecting brain regions intrinsically linked with cognition are present in the D409V/WT mice. In the absence of Lewy body deposition, the D409V/WT mice could be considered an early pre-clinical model of LBD with potential for drug discovery. Since few robust pre-clinical models of LBD currently exist, with further characterization, the mouse model described here may contribute significantly to developments in the LBD field.

1. Introduction

In the 20 years since mutations in the *GBA1* gene, coding for the lysosomal hydrolase glucocerebrosidase, were first linked to the development of parkinsonian symptoms (Neudorfer et al., 1996), genetic testing has established heterozygous mutations in *GBA1* as the most common genetic risk factor for Parkinson's disease (PD) (Sidransky et al., 2009).

While overt pathological differences between *GBA1* associated PD (GBA-PD) and sporadic PD have not been described thus far (Neumann et al., 2009; Parkkinen et al., 2011; Westbroek et al., 2011), earlier age of onset by approximately 6 years (Gan-Or et al., 2008; Neumann et al., 2009; Nichols et al., 2009) and more rapid disease progression (Winder-Rhodes et al., 2013; Beavan et al., 2015; Davis et al., 2016) are widely reported. Perhaps one of the most striking clinical findings has been that GBA-PD patients are 5 times more likely to develop cognitive impairment and dementia (PD dementia) compared with sporadic PD patients (Goker-Alpan et al., 2008; Neumann et al., 2009; Sidransky et al., 2009; Brockmann et al., 2011; McNeill et al., 2012; Seto-Salvia et al., 2012; Chahine et al., 2013; Beavan et al., 2015; Jesus et al., 2016; Lunde et al., 2018; Simitsi et al., 2018) with the presence of a *GBA1* mutation reported to be a significant predictor of progression of dementia (Neumann et al., 2009; Winder-Rhodes et al., 2013). In accordance with these findings, the presence of a mutant *GBA1* allele has

Abbreviations: GCase, Glucocerebrosidase; GluCer, glucosylceramide; LBD, Lewy body dementia; DG, Dentate gyrus; MWM, Morris water maze; vAChT, Vesicular acetylcholine transporter; CHAT, Choline acetyltransferase; SPP, Synaptophysin

* Corresponding author.Wolfson Centre for Age-Related Diseases, King's College London, London, SE1 1UL, UK.
E-mail address: Emily.clarke@kcl.ac.uk (E. Clarke).

https://doi.org/10.1016/j.neuint.2019.104502
Received 15 April 2019; Received in revised form 21 June 2019; Accepted 8 July 2019
Available online 09 July 2019

also been significantly linked with increased risk of developing dementia with Lewy bodies (DLB) (Goker-Alpan et al., 2006; Nalls et al., 2013; Guerreiro et al., 2018).

Neuropathology associated with Lewy body dementia (LBD) (dementia with Lewy bodies and Parkinson's disease dementia) is principally defined by the intraneuronal deposition of aggregated insoluble α-synuclein in the form of Lewy bodies and Lewy neurites. However, common pathologies associated with Alzheimer's disease, neurofibrillary tangles composed of tau and neuritic plaques composed of Aβ are also frequently found in the brain of patients. Revealingly, extensive cholinergic deficits often associated with the basal forebrain occur relatively early in the disease course of LBD and have become established as a differentiating factor from Alzheimer's disease(Jellinger, 2018). Hall et al. comprehensively report the association between hippocampal Lewy pathology and cholinergic dysfunction in human post mortem Parkinson's disease dementia brain (Hall et al., 2014).

GBA1 encodes the lysosomal hydrolase glucocerebrosidase (GCase) which is involved in glycosphingolipid metabolism(Ginns et al., 1985). The principal substrate of *GBA1* derived GCase is glucosylceramide (GluCer). The lysosomal storage disorder Gaucher's disease is caused by *homozygous* mutations in *GBA1* and is characterised by accumulation of GluCer as a consequence of dramatically reduced *GBA1* GCase enzyme activity (Grabowski, 2008). Post mortem studies report reduced *GBA1* GCase enzyme activity in sporadic PD and DLB brain in key regions related to symptom development such as the substantia nigra and anterior cingulate cortex (Gegg et al., 2012; Chiasserini et al., 2015; Rocha et al., 2015a,b; Moors et al., 2019). Furthermore, reduced levels of *GBA1* GCase activity in these brain regions is associated with increased α-synuclein levels (Gegg et al., 2012; Murphy et al., 2014). More recently, it has been uncovered that GCase enzyme activity progressively declines with age in healthy brain (Rocha et al., 2015a,b; Hallett et al., 2018) which is hugely significant since aging is the biggest single risk factor for the development of LBD.

GBA1 investigations in rodents have traditionally been performed by pharmacological inhibition of GCase enzyme activity, conditional knockout of *GBA1* or breeding homozygous *GBA1* mutant mice. The pathology and symptoms of Gaucher's disease is recapitulated due to a drastic and early reduction in GCase activity. Interestingly, cognitive impairment has been reported in a mouse model of Gaucher's disease expressing homozygous knock in point mutations in *GBA1* – D409V/D409V (Sardi et al., 2011). Accompanying this phenotype, pathogenic hallmarks of LBD, ubiquitin positive α-synuclein aggregates and tau aggregates were also identified in the hippocampus (Sardi, Clarke et al. 2011, 2013). We believe that heterozygous D409V/WT *GBA1* mice would be a more translational model of LBD for 3 main reasons. First, heterozygous, not homozygous mutations in *GBA1* are associated with LBD. Second, the reduction in brain GCase enzyme activity in D409V/WT *GBA1* mice more accurately reflects brain GCase enzyme activity in both GBA-PD and sporadic PD patients (Gegg et al., 2012; Kurzawa-Akanbi et al., 2012; Murphy et al., 2014; Clark et al., 2015; Rocha et al., 2015a,b). Third, a mouse model which demonstrates age related decline in symptomology better reflects clinical representation of LBD patients rather than severe pathology and symptoms at an early age.

We therefore investigated the impact of age/continuing exposure of D409V/WT *GBA1* mutation on mouse brain focussing on neurochemical, pathological and behavioural indices relevant to LBD to evaluate the translational potential of this model for drug discovery. Accordingly, we decided to functionally assess D409V/WT *GBA1* mice for cognitive impairment at 3, 6, 9 and 12 months of age in order to consider the impact of the previously reported progressive decline in GCase enzyme activity with aging(Hallett et al., 2018) and identify any age related decline in cognitive ability mirroring the clinical development of LBD. Additionally, we biochemically analysed brain tissue to assess α-synuclein aggregation, glial proliferation and cholinergic integrity – characteristic pathological hallmarks of LBD.

This paper presents evidence to suggest that D409V/WT *GBA1* mice at 12 months of age may provide a pre-Lewy body model of LBD. The added impact of aging further reduces hippocampal GCase enzyme activity causing an age-related decline in cognitive function. Furthermore, aging of D409V/WT mice uncovers pathological features of LBD namely glial proliferation and cholinergic dysregulation in the brain. These pathological responses could potentially underlie cognitive deficits in the absence of motor impairment. This model, while requiring further in-depth study, has great potential for drug discovery and testing for LBD.

2. Materials and methods

2.1. Animals

D409V/D409V *GBA1* mice (stock number 019106) were purchased from The Jackson Laboratory (Maine, USA) and crossed with C57Bl/6 wild type mice to generate D409V/WT *GBA1* heterozygotes. Male mice were maintained in a 12-h light dark cycle at ambient temperature and humidity with *ad libitum* access to food and water. All mice were maintained, procedures performed and culled by cervical dislocation in accordance with UK Animals (Scientific Procedures) Act 1986.

2.2. Behavioural tests

2.2.1. Morris Water Maze

The Morris water maze task was performed as previously described (Vorhees and Williams, 2006). Briefly, a 130 cm diameter water maze was filled with water and left to equilibrate to room temperature overnight. A platform, submerged 1 cm below the water line was placed in a designated quadrant. Mice were introduced to the water maze to search for the platform for a maximum of 90 s. Mice which failed to find the platform were placed on the platform for 10 s to allow for environmental familiarisation. 4 trials starting from different points of the maze (north, east, south or west) were performed at 30-min intervals. Testing was performed for 5 consecutive days to generate learning curves. 24 h following the final trial, the platform was removed, and mice explored the water maze for 60 s constituting the probe trial.

2.2.2. Y-maze

The protocol for Y-maze testing and spontaneous arm performance was based upon paradigms described by Deacon et al.(Deacon and Rawlins, 2006) and Hughes et al.(Hughes, 2004). Briefly, mice were placed in the centre of a Y-maze and allowed to explore the arms of the maze for 8 min. The arms of the maze measured 35 cm in length and 4 cm in diameter. The maze was cleaned with ethanol between trials and lighting was even across the maze. The recording of each trial was manually scored for the number of spontaneous arm entries – the total number of correct triad arm entries attempted within 8 min. The % of spontaneous arm entries was calculated.

2.2.3. Open field

Open field testing was carried out as previously described (Seibenhener and Wooten, 2015). Briefly, mice were habituated to the testing room 30 min before testing, Mice were placed in a 45 cm^2 open field arena for 20 min and allowed to explore. Lighting across the arena was even and the area cleaned with ethanol between trials. Trails were recorded by video camera and analysed using EthoVision XT version 11 software (Noldus, Netherlands). The arena was calibrated using the EthoVision software to reflect the dimensions in addition to the presence of a 11.25 cm^2 square border. The following parameters were measured: distance covered (cm); velocity (cm/s) and time spent in the border (s).

2.2.4. Rotarod

Motor performance was evaluated on a 5-lane rotarod unit as previously described(Fleming et al., 2013). Mice were pre-trained by

placing them on the rod that was set to accelerate from 4 to 40 rpm over a period of 5 min. If the mice fell off under 1 min, they were placed back on the rotarod during training. Mice were pre-trained twice a day for 3 days, with a 1-h rest between each session. On the fourth day, mice were tested twice using the same protocol, with the average latency to fall being recorded between both sessions.

2.3. Lysosomal enzyme activity assay

Mouse brain tissue was homogenised as a 5% homogenate in H_2O and assayed for protein concentration using Pierce Bradford assay kit (Thermo Fisher Scientific, USA) and normalised to 2 mg/ml. GCase enzyme activity was measured as described previously using the artificial substrate 4-methylumbelliferone-β-glucopyranoside (4-MUP) (Sigma Aldrich, USA) at 10 mM in McIlvaine buffer pH 5.4(Burke et al., 2013). Activated *GBA1* derived GCase activity was assessed by incubating samples in 4-MUP substrate in the presence of 9.3 mM sodium taurocholate which acts to activate *GBA1* GCase enzyme. *GBA2* derived GCase activity was assessed by performing incubations of samples in 4-MUP substrate in the presence and absence of 2.5 μM deoxynojirimycin (DNJ), a specific inhibitor of *GBA2* derived GCase enzyme activity (Sigma Aldrich, USA), and calculating the difference in activity. All incubations took place at 37 °C for 60 min. Reactions were stopped by the addition of 1 mL 0.25M glycine (Sigma-Aldrich, USA) pH10.4. Cleaved fluorescent 4-methylumbelliferone was measured using a spectrophotometer (Flexstation II, Molecular Devices, USA) excitation 365 nm, emission 450 nm.

β-galactosidase activity was measured in the same sample preparations of brain homogenate prepared as described above. 0.4% human serum albumin (Sigma Aldrich, USA) and 0.4 M sodium chloride (Sigma Aldrich, USA) were added to sample and incubated in 1 mM of the artificial enzyme substrate 4-methylumbelliferyl-β-D-galactopyranoside (4-MUG) (Sigma-Aldrich, USA) in McIlvaine buffer pH 4.1. The reaction was incubated 37 °C for 15 min. The reaction was stopped by addition of 0.25M glycine pH10.4 and cleaved fluorescent 4-methylumbelliferone measured as described above(Burke et al., 2013).

2.4. Gene expression

Quantitative PCR was performed as previously described(Medhurst and Pangalos, 2003). Briefly, RNA was converted to cDNA using Applied Biosystems™ high capacity RNA-to-cDNA™ kit (Applied Biosystems™, USA) as per manufacturer's instructions. Pre-designed housekeeping and gene of interest primers and fluorescent probes in the form of TaqMan® Gene Expression Assays were purchased from Applied Biosystems™: Mm02619580_g1(ActB), Mm01221880_m1(CHAT), Mm00436850_ma(Synaptophysin) and Mm00491465_s1(vAChT). Threshold values (C_t) values were compared to ActB housekeeping gene using the $\Delta\Delta^{ct}$ method(Livak and Schmittgen, 2001) to give a value of relative gene expression.

2.5. Immunofluorescence

Brains were removed and hemisected. One hemisphere was post fixed in 4% paraformaldehyde prior to sagittal embedment in paraffin. Brain was sectioned using a microtome into 7 μm sections. Sections were dewaxed with Histo-Clear (National Diagnostics, USA) and subsequently rehydrated with graded dilutions of ethanol (100%, 90% and 70%). Antigen retrieval was performed by microwaving sections in preboiled 0.01M citrate buffer pH6.4 for 5 min. Slides were washed in PBS, 3 × 3 min before incubation with primary antibody overnight at 4 °C. Primary antibodies used were: anti-vAChT rabbit polyclonal antibody (synaptic systems, 139 103, Germany) at 1:4000, anti-ChAT goat polyclonal antibody (EMD Millipore, AB144P, USA) at 1:500 and anti-synaptophysin mouse monoclonal clone SY38 antibody (Abcam, ab8049, UK) at 1:150. Sections were washed with PBS 3 × 3 min and then incubated at room temperature with fluorescent secondary antibodies for 90 min: AlexaFluor® donkey anti-rabbit 568 nm, Alexa Fluor® donkey anti-goat 647 nm, and Alexa Fluor® donkey anti-mouse 488 nm (Thermo Fisher Scientific, USA) at 1:500. Secondary antibody was discarded and 300 nM DAPI solution (Thermo Fisher Scientific, USA) was applied to sections for 3 min. Slides were washed in PBS, 3 × 3 min and incubated in Sudan Black (0.1% in 70% ethanol) for 20 min at room temperature. Slides were washed under running tap water and mounted in Vectamount™ AQ mounting media (H-5501, Vector Laboratories, USA). Staining was imaged using a Zeiss LSM 710 confocal microscope and Zeiss ZEN lite software.

Image processing and quantification were performed in ImageJ2 software (NIH) on Fiji platform as follows. Pixels containing immunoreactive signals of endogenous mouse IgG by secondary anti-mouse 488 in blood vessels were first excluded from a polygonal selection which encompassed a part of the dentate gyrus within each field. The same blood vessel-free selection was used for each image channel from the same field. Non-specific background signals and unequal lighting in each image channel were eliminated with *Subtract Background* function. Synaptophysin was quantified as mean grey value since the entire molecular layer of the DG is covered with synaptophysin-positive puncta. For each vAChT or ChAT image, a threshold value (to highlight any pixels with grey value from X to 255) that yielded the peak average particle size was applied to conceptually maximise the staining area of axons and minimise digital noises. Cholinergic axon staining was quantified as a percentage of the total area of all particles larger than 2 pixels highlighted by the threshold over the area of the blood vessel-free selection.

2.6. 3-3′-diaminobenzidine (DAB) staining

DAB staining was performed with sections prepared as described above for immunofluorescence. Antigen retrieval for Iba1 and GFAP was performed by microwaving in 0.01M citrate buffer pH6.0 for 10 min while antigen retrieval for α-synuclein was carried out by autoclaving for 10 min in EDTA buffer pH8.0 followed by immersion for 15 min in 98% formic acid. The following primary antibodies used were: Iba1 at 1:2000 (Wako Pure Chemical Industries, Japan); GFAP at 1:8000 (DAKO, Agilent Technologies, UK); α-synuclein ab27766 at 1:200 (Abcam, UK); α-synuclein ab1903 at 1:500 (Abcam, UK); and α-synuclein phosphor-serine129 ab51253 at 1:500 (Abcam, UK). Despite indications of human species specificity for ab27766, analysis of the epitope recognition site and amino acid sequence suggests cross reactivity with mouse which was confirmed. After overnight incubation, sections were incubated at room temperature with biotinylated goat anti-rabbit secondary antibody (Vector laboratories, USA) at 1:500. The ABC elite kit (Vector Laboratories, USA) was used for detection of biotinylated secondary antibodies and colour developed using the DAB Peroxidase (HRP) substrate kit with nickel (Vector Laboratories, USA). Tissue was counterstained with Mayer's Haematoxylin (Sigma-Aldrich, USA) before dehydration with decreasing dilutions of alcohol and xylene. Sections were coverslipped using DPX mountant (Sigma-Aldrich, USA) and allowed to dry prior to imaging using Leica DMRB equipped with DC420 digital camera. Image analysis was conducted using ImageJ2 software (NIH) on Fiji platform.

2.7. Western blotting

Western blotting was performed as previously described. Briefly, samples were homogenised using the IKA Ultra Turrax hand held homogeniser as a 10% w/v solution in ddH20 with Complete EDTA free protease inhibitors (Roche, Switzerland) and PhosSTOP tablets (Roche, Switzerland). Homogenate was aliquoted and stored at −20 °C until requires. Protein concentration was determined using Pierce Coomassie protein assay kit (Thermo Fisher Scientific, United States) as per manufacturer's instructions. All homogenates were normalised to 1 mg/mL

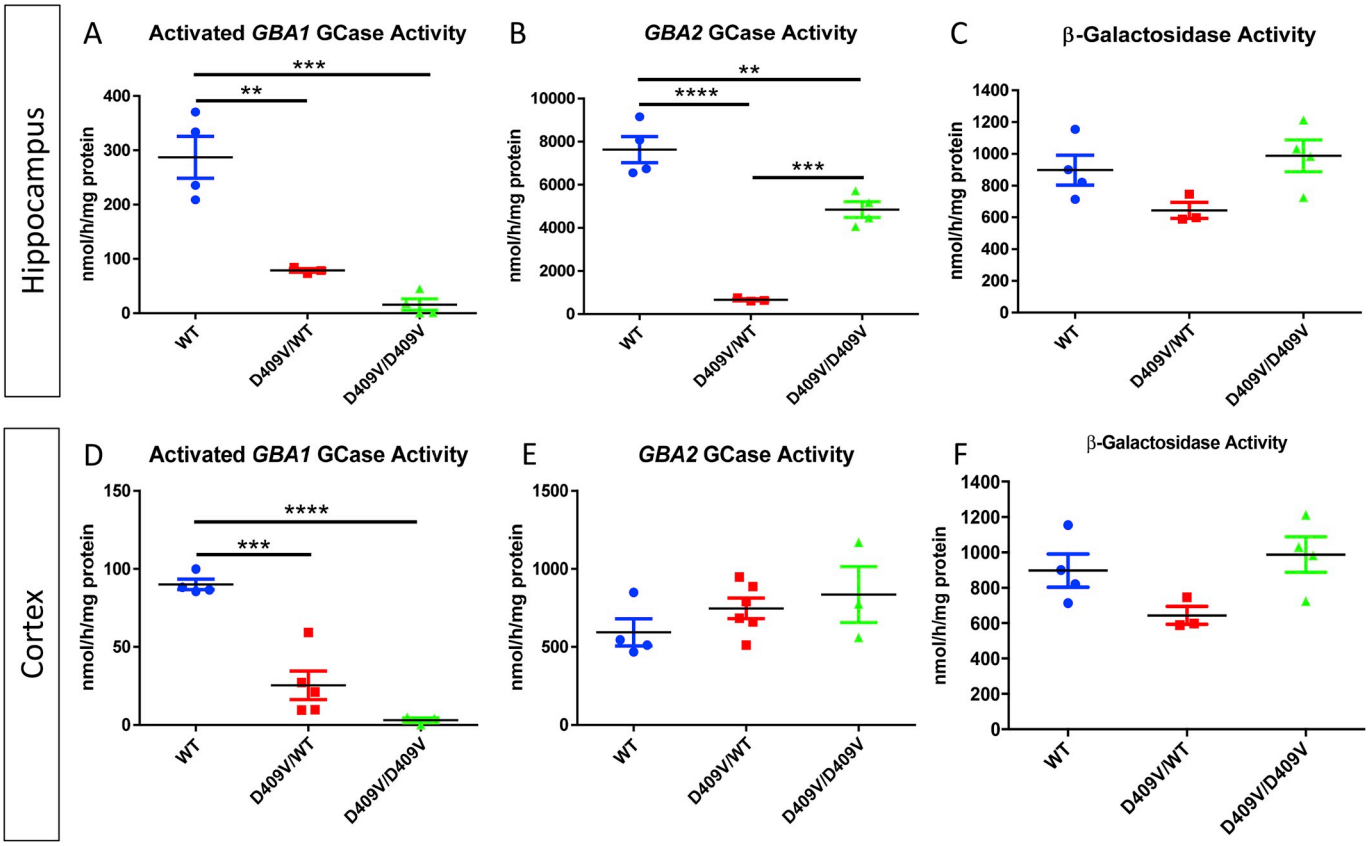

Fig. 1. Brain GCase Enzyme Activity in D409V Mutant Mice at 12 months
(a) Activated *GBA1* GCase activity in the hippocampus, One-way ANOVA, Tukey's HSD, F(2,8) = 32.80,**p = 0.0014, ***p = 0.0001
(b) *GBA2* GCase activity in the hippocampus, One-way ANOVA, Tukey's HSD, F(2,8) = 54.58, ****p = 0.00001,**p = 0.0050,***p = 0.0006
(c) β-galactosidase activity in the hippocampus, One-way ANOVA, F(2,8) = 3.469, p = 0.082,
(d) Cortical activated *GBA1* GCase enzyme activity, One way ANOVA, F(2,9) = 37.73, Tukey's HSD, ****p = 0.00001 ***p = 0.0002
(e) Cortical *GBA2* GCase enzyme activity, One way ANOVA, F(2,10) = 1.32, p = 0.3099
(f) Cortical β-galactosidase enzyme activity, One-way ANOVA, F(2,8) = 1.091, p = 0.3812. All data represented as mean enzyme activity ± SEM, n = 3–4 mice per group.

and boiled in SDS-PAGE loading buffer (2B scientific, UK) for 5 min (except samples for vAChT which were not boiled according to antibody datasheet). 20 µg of protein was loaded per well in a 10% Tris gel. Proteins were transferred onto nitrocellulose membrane (GE Healthcare, United States) and the membrane blocked with 10% milk/PBS-Tween 0.05% solution for 1 h. Primary antibody was constituted in 5% milk/PBS-Tween 0.05% solution and added to the membrane to incubate overnight at 4 °C. Primary antibodies were used at the following concentrations: rabbit anti-GBA 1:1000 (Abcam ab175869, UK); goat anti-CHAT 1:650 (EMD Millipore AB144P, USA); rabbit anti-vAChT 1:1000 (Synaptic Systems 139 103, Germany); rabbit anti-GAPDH 1:25000 (Abcam ab9485, UK); rabbit anti-β Tubulin 1:10,000 (Abcam ab6046) and goat anti-GAPDH 1:1000 (Abcam ab9483, UK). Primary antibody solution was removed, and the membrane washed 3 × 5mins with PBS-Tween 0.05% prior to incubation with fluorescent secondary antibody prepared in 5% milk/PBS-Tween 0.05% at room temperature for 1 h. The following secondary antibodies were used: Alexa Fluor goat anti-rabbit 1:5000 (Molecular Probes, USA) and Alexa Fluor rabbit anti-goat 1:5000 (Molecular Probes, USA). Secondary antibody solution was removed, and the membrane washed 3 × 5 min with PBS-Tween 0.05%. Protein bands were visualised using the Li-Cor Odyssey Infrared scanner. Band densities were quantified using Li-Cor Image Studio Lite software.

2.8. Meso Scale Diagnostics sandwich immunoassay

Hippocampi were dissected from fresh frozen tissue and homogenised in PBS. Protein concentration was determined by Coomassie protein assay kit (Thermo Fisher Scientific, United States) as per manufacturer's instructions. All homogenates were normalised to 1 mg/mL. Sandwich immunoassay was performed as per manufacturer's instructions. Briefly, α-synuclein capture antibody (Synaptic systems 128 211, 1 µg/ml, Germany) was immobilised onto a working electrode within a well of a 96-well plate via the U-PLEX linker provided. Samples and controls were added to wells and incubated at room temperature for 1 h with shaking. After washing with MSD wash buffer, capture antibody (Synaptic systems 128 003, 1 µg/ml, Germany) conjugated with electrochemiluminescent label (MSD Sulfo Tag) was added completing the immunoassay sandwich. The plate was washed, and MSD read buffer added for the plate to be analysed by MSD MESO QuickPlex SQ 120 instrument.

2.9. Statistical analysis

Statistical analyses were performed by One-way ANOVA followed by Tukey's HSD post hoc test for enzyme activity assays. Morris water maze learning curves underwent repeated measures Two-way ANOVA followed by Sidak post hoc test. Morris water maze probe trial at 12 months was statistically analysed by student's t-test. Performance over 12 months in Y-maze was subject to repeated measures Two-way

ANOVA followed by Sidak post hoc test. Quantification of immunofluorescent and immunohistochemical staining was analysed by student's t-test. Western blot data was analysed by One-way ANOVA while gene expression data was analysed by Two-way ANOVA followed by Bonferroni correction.

Statistical analyses were performed All statistical analyses were performed using GraphPad Prism v7.0 (GraphPad Software). Values with $P < 0.05$ were considered significant.

3. Results

D409V/WT *GBA1* mice demonstrate a significant reduction in activated *GBA1* derived GCase enzyme activity in the brain compared with WT.

Activated *GBA1* derived GCase enzyme activity was significantly reduced by 72.57% in the hippocampus of D409V/WT mice compared with wild type at 12 months (D409V/WT = 78.78 ± 3.342, WT = 287.2 ± 38.68 nmol/h/mg protein) (Fig. 1a). Activated *GBA1* activity in the cortex of the same animals was reduced by 71.79% (D409V/WT = 25.42 ± 9.115, WT = 90.10 ± 3.339 nmol/h/mg protein) at 12 months of age (Fig. 1d). In both the hippocampus and cortex GCase enzyme activity is almost ablated in homozygous D409V/D409V mice by 94.45% (Figs. 1a) and 96.67% (Fig. 1d) respectively. In all cases, β-galactosidase enzyme activity does not change between genotype or brain region (Fig. 1c **and** f). Furthermore, GCase protein expression is not altered between genotype (Fig. S1).

D409V/WT GBA1 mice have significantly reduced *GBA2* derived GCase activity in the hippocampus but not the cortex compared with both WT and D409V/D409V homozygous *GBA1* mice.

Hippocampal *GBA2* derived GCase enzyme activity is highly significantly reduced by 91.4% (D409V/WT = 662.1 ± 81.52, WT = 7629 ± 610.2 nmol/h/mg protein) in 12 months D409V/WT *GBA1* mice when compared with WT (Fig. 1b). Interestingly, *GBA2* derived GCase enzyme activity recovers in the D409V/D409V homozygotes to 63.5% of WT activity (D409V/D409V = 4846 ± 36.8, WT = 7629 ± 610.2 nmol/h/mg protein) (Fig. 1b).

GBA2 derived GCase enzyme activity is over 20 times greater than activated *GBA1* GCase in the hippocampi of WT mice and 8 times greater in D409V/WT mice (Fig. 1a and b). Furthermore, both *GBA1* and *GBA2* derived GCase activity is significantly greater in the hippocampus when compared with cortical activity (Fig. 1a,b,d,e).

D409V/WT *GBA1* mice demonstrate an age-related decline in cognitive performance reaching significance by 12 months of age in the absence of motor deficits or evidence of anxiety.

Learning was demonstrated by both wild type and D409V/WT *GBA1* mice in the water maze at 3, 6, and 9 months of age as seen by a steady improvement in both trial duration and distance to platform over the 5 consecutive trial days (Fig. 2a,b,c). However, by 12 months of age, performance of D409V/WT *GBA1* mice plateaus and at day 5 of training there is significantly worse performance for both trial duration (D409V/WT = 45.57 ± 8.12 s, WT = 17.79 ± 2.66 s)(Fig. 2d) and

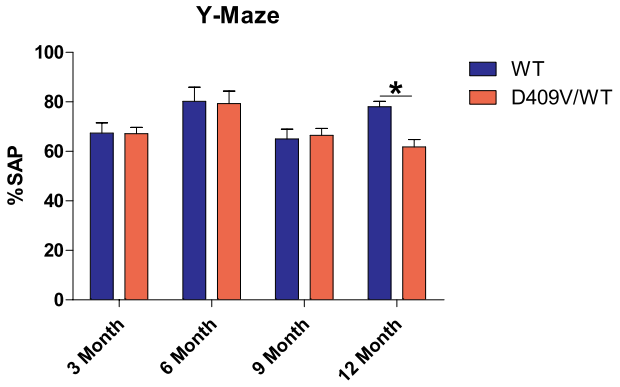

Fig. 3. Spontaneous Alternation Performance in a Y-Maze of D409V/WT Mice. Data represented as mean spontaneous alternation performance ± SEM, Repeated measures ANOVA, Sidak's post hoc test, F(3,42) = 4.591, *p = 0.02, n = 8–10 mice per group.

distance to platform (D409V/WT = 651.07 ± 121.83 cm, WT = 257.07 ± 46.38 cm) (Fig. S2a) in the absence of any discernible alteration in swim velocity (Fig. S2b), indicating cognitive impairment. Cognitive impairment at 12 months of age was confirmed by probe trial with D409V/WT mice spending significantly less time in the quadrant which previously contained the platform (11.57 ± 1.62 s) compared with wild type (17.87 ± 2.29 s) (Fig. 2e).

The percentage spontaneous alternation performance (%SAP) measured by Y-maze testing showed similar cognitive performance when executing the task at 3, 6 and 9 months of age when D409V/WT *GBA1* mice were compared with age matched controls (Fig. 3). By 12 months of age, there is a significant reduction in % SAP indicative of cognitive impairment in D409V/WT mice (WT = 78.53 ± 2.38%, D409V/WT = 60.87 ± 3.22%, repeated measures ANOVA, Sidak's post hoc test, F(3,42) = 4.591, n = 9 per group, *p = 0.0189).

The absence of a motor deficit at 12 months of age was confirmed by rotarod. There was no significant difference in latency to fall between wild type (160.6 ± 32.01s), D409V/WT (180.6 ± 31.17s) and D409V/D409V mice (128 ± 20.32s) (One way ANOVA, F(2,14) = 0.643, p = 0.540) indicating the absence of a motor deficit (Fig. S3c). Furthermore, there was no difference in the distance travelled or speed as measured in an open field arena over 20 min (Figs. S3a and b). There was also no evidence of anxiety as measured in the % time spent in the perimeter of the open field arena (WT = 89.78 ± 1.79%, D409V/WT = 90.86 ± 1.43%) (Fig. S3d).

D409V/WT *GBA1* mice do not show increased deposition of Lewy bodies in the hippocampus by immunohistochemistry but ELISA indicates a subtle but not statistically significantly increase in soluble monomeric α-synuclein.

Standard immunohistochemical analysis of hippocampal sections using two independent α-synuclein antibodies – Abcam ab1903 mouse monoclonal [4D6] antibody and Abcam ab27766 mouse monoclonal

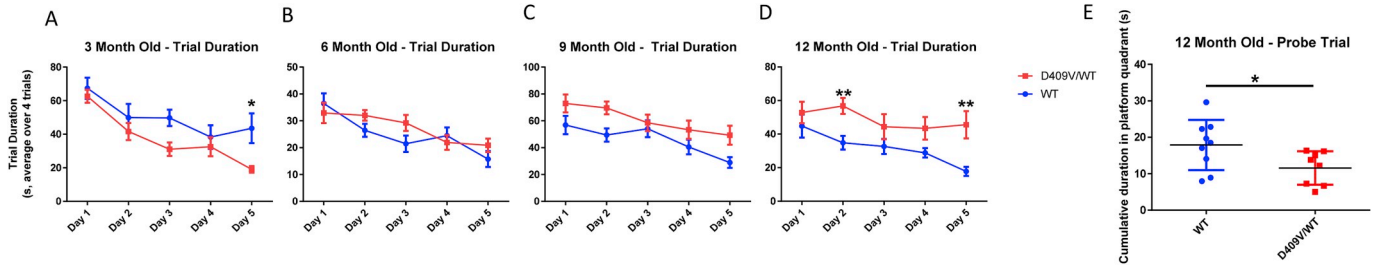

Fig. 2. Morris Water Maze in D409V/WT *GBA1* mice. Learning curves showing duration in seconds to submerged platform over 5 consecutive days in (a) 3 months old (b) 6 months old, (c) 9 months old and (d) 12 months old D409V/WT and age matched WT mice. Data represented as mean trial duration ± SEM, Repeated measures Two-way ANOVA, Sidak post hoc test (e) Probe trial at 12 months old. Data represented as mean duration ± SEM, student's t-test, *p = 0.04, n = 9/8 mice per group.

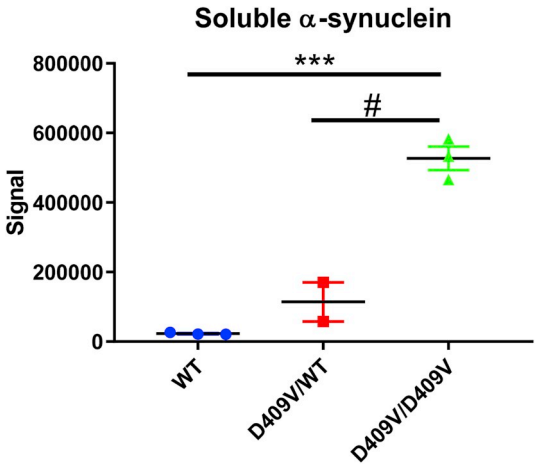

Fig. 4. Hippocampal α-synuclein sandwich immunoassay quantification of soluble α-synuclein at 12 months of age. Data expressed as mean intensity ± SEM, One way ANOVA, F(2,5) = 79.21, Tukey's HSD, ***p = 0.0002, #p = 0.0007, n = 3 mice per group except D409V/WT where n = 2 mice per group.

[LB 509] antibody - failed to detect any α-synuclein aggregates/Lewy body staining of note in either D409V/WT *GBA1* hippocampus or wild type controls at 12 months of age (Fig. S4). There was also no phosphorylated 129 α-synuclein staining of note (data not shown).

Meso Scale Diagnostics sandwich immunoassay for soluble α-synuclein in the hippocampus of 12 months old mice shows a highly significant increase in α-synuclein present in the hippocampus of D409V/D409V mice (527238 ± 34000) compared with both WT (22904 ± 1706) and D409V/WT (114156 ± 56188) (One-Way ANOVA, F(2,5) = 79.21, Tukey's HSD,***p = 0.0002(WT), ***p = 0.0007(D409V/WT). While increased, the quantification of α-synuclein in the hippocampus of D409V/WT mice compared with WT is not significant (p = 0.22) (Fig. 4).

D409V/WT *GBA1* mice have increased staining for astrocytes and microglia in the hippocampus at 12 months.

The total number of GFAP positive cells in the hippocampus is significantly increased in D409V/WT mouse brain when compared with WT (WT = 162 ± 36.01, D409V/WT = 317.78 ± 42.73, student's t-test, **p = 0.0028) (Fig. 5a and b). The percentage area of Iba1 staining in the same animals also showed a significant increase in the hippocampus of D409V/WT mice (WT = 7.86 ± 2.09, D409V/WT = 23.92 ± 2.16, student's t-test, ****p = 0.0001) (Fig. 5c and d).

Cholinergic deficits are evident in the hippocampus of D409V/WT *GBA1* mice at 12 months of age.

At the protein level, immunofluorescence also indicates a highly significant 69.4% reduction in vAChT percentage staining area in the dentate gyrus of D409V/WT mice at 12 months (WT = 0.76 ± 0.09%, D409V/WT = 0.23 ± 0.05%, student's t-test, ***p = 0.0001, n = 9 per group) (Fig. 6a,c). A similar but not significant trend is also seen by Western blot (WT = 0.121 ± 0.022, D409V/WT = 0.070 ± 0.11, D409V/D409V = 0.084 ± 0.018. One way ANOVA, F(2,6) = 2.214, p = 0.022, n = 3 per group) (Fig. 7a and b).

CHAT immunofluorescence in the dentate gyrus shows a significant 31.8% increase in staining percentage area in D409V/WT mice compared with wild type at 12 months (WT = 1.71 ± 0.08%, D409V/WT = 2.47 ± 0.24%, Student's t-test, *p = 0.010) (Fig. 6a,d). Nevertheless, semi-quantitative Western blot of hippocampal tissue does not show any significant change in CHAT protein expression in *GBA1* mutant mice compared with wild type (WT = 0.144 ± 0.033, D409V/WT = 0.116 ± 0.171, D409V/D409V = 0.173 ± 0.046. One way ANOVA, F(2,6) = 2.096, p = 0.204, n = 3 per group) (Fig. 7a,c).

When expressed as a ratio to represent the density of functional vAChT positive boutons on CHAT positive axons, VAChT/CHAT protein expression ratio by immunofluorescence shows a highly significant 78.3% reduction in D409V/WT dentate gyrus compared with wild type (WT = 0.40 ± 0.03%, D409V/WT = 0.09 ± 0.01%, Student's t-test ****p= < 0.0001, n = 9 per group) (Fig. 6a,e). These alterations to cholinergic protein expression are reported in the background of significantly reduced immunofluorescent staining for synaptophysin by 42.1% (WT = 1.43 ± 0.21, D409V/WT = 0.83 ± 0.14, Student's t-test *p = 0.03) (Fig. 6a and b).

Relative gene expression of *SLC18A3* (vAChT) is significantly reduced in the hippocampus of D409V/WT *GBA1* mice at 12 months compared with wild type (WT = 1.00 ± 0.26, D409V/WT = 0.21 ± 0.026, Two-way ANOVA with Bonferroni correction, F(1,18) = 24.77, *p = 0.011). Gene expression of CHAT is also significantly reduced (0.088 ± 0.24 compared with 1.00 ± 0.23, Two-way ANOVA with Bonferroni correction, F(1,18) = 24.77, **p = 0.0034). Reductions in both vAChT and CHAT relative gene expression are seen in the absence of any significant change in *SYP1* (synaptophysin) expression (Fig. 7d).

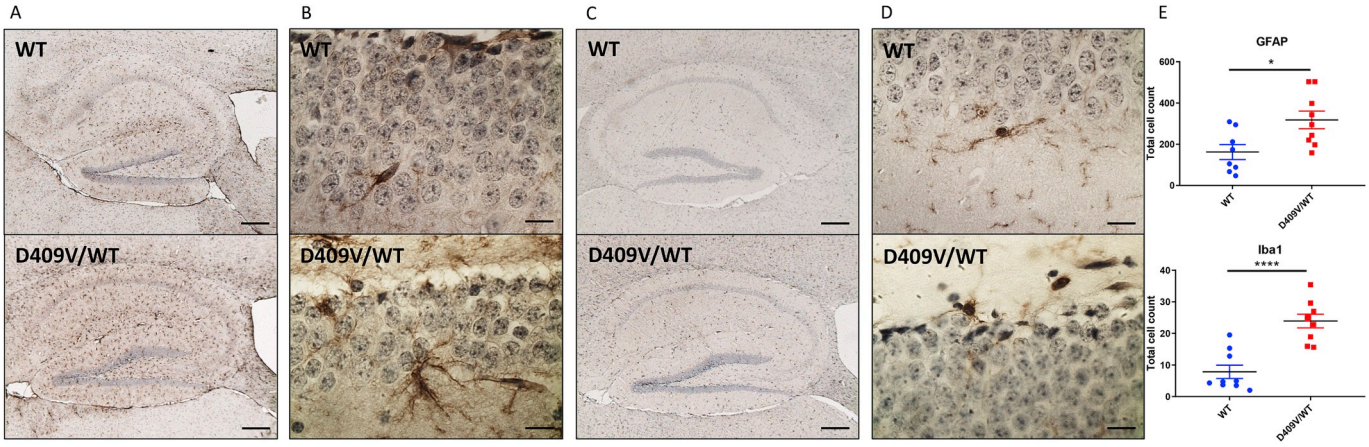

Fig. 5. Hippocampal GFAP and Iba1 staining at 12 months (a) Representative images of GFAP staining in the hippocampus of D409V/WT and WT mice. Scale bar = 200 μM (b) Representative images of GFAP staining in the dentate gyrus of D409V/WT and WT mice. Scale bar = 20 μM (c) Representative images of Iba1 staining in the hippocampus of D409V/WT and WT mice. Scale bar = 200 μM (d) Representative images of Iba1 staining in the dentate gyrus of D409V/WT and WT mice. Scale bar = 20 μM (e) Quantification of GFAP positive cell count and Iba1 positive cell count in the dentate gyrus. Data expressed as mean total cell count ± SEM, Student's t-test, *p = 0.0149,****p= < 0.0001, n = 9 per group.

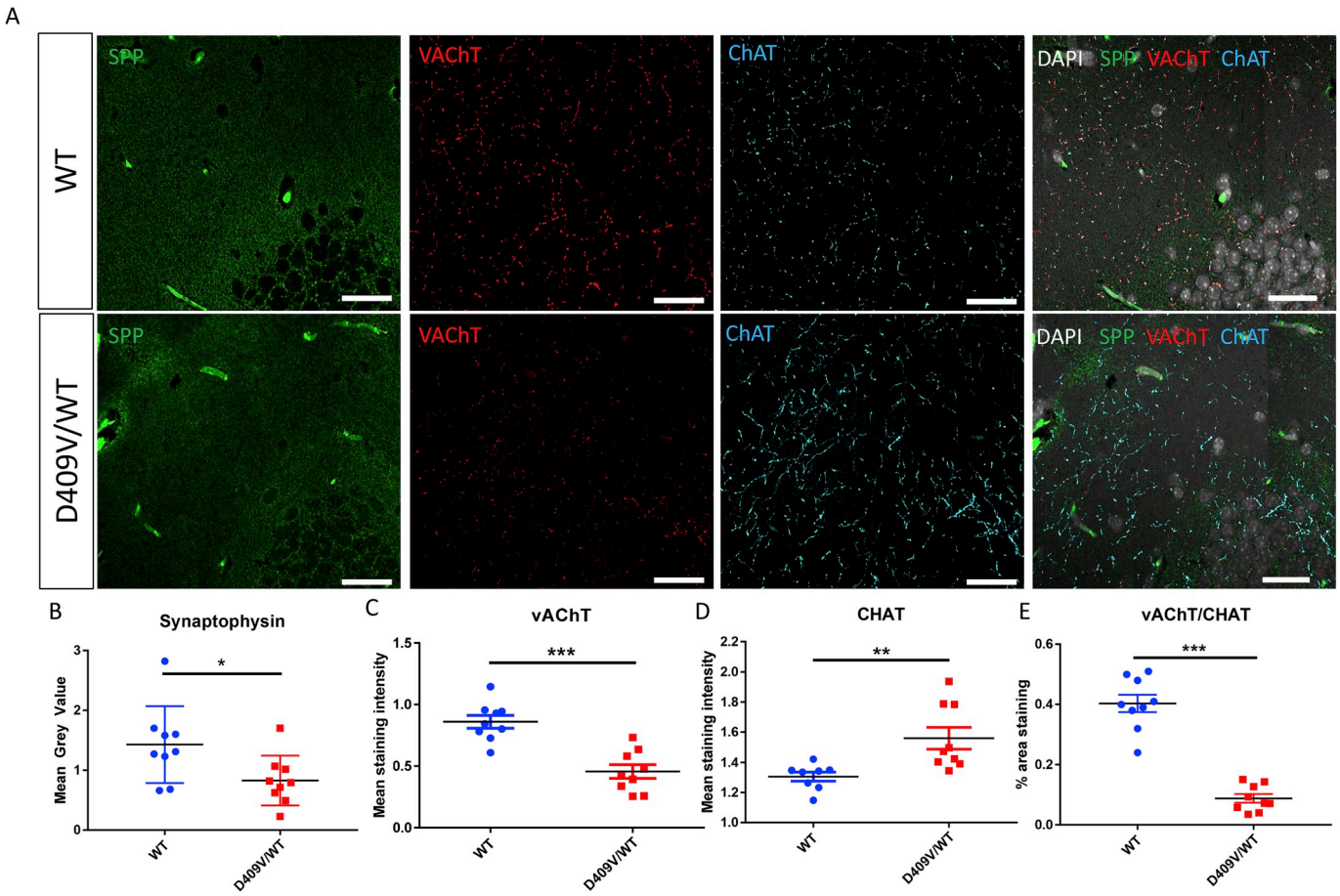

Fig. 6. Altered cholinergic protein expression in the hippocampus of D409V/WT mice by immunofluorescence (a) Representative images of synaptophysin (green), vAChT (red),CHAT (blue) and DAPI (white) immunofluorescent staining in the dentate gyrus of D409V/WT and WT mice at 12 months. Scale bar = 40 μM (b) Quantification of synaptophysin staining. Data expressed as mean grey area ± SEM. Student's t-test, *p = 0.0317 (c) Quantification of vAChT staining. Data expressed as mean grey value ± SEM, student's t-test, ***p = 0.0001 (d) Quantification of CHAT staining. Data expressed as mean staining intensity ± SEM, student's t-test,**p = 0.0072 (e) ratio of vAChT/CHAT staining, student's t-test. n = 9 mice per group.

4. Discussion

This study demonstrates the novel finding of age-related cognitive impairment in heterozygous D409V/WT *GBA1* mutant mice. The translational potential of this mouse model for the study of LBD is further evidenced by equivalent reductions in brain *GBA1* derived GCase enzyme activity as seen in both *GBA1* mutant and sporadic PD and DLB brain. Evidence of glial proliferation and cholinergic deficits involving the hippocampus of 12 months old D409V/WT mice, pathological features of LBD, provides further support for the translational value of this mouse model despite the apparent lack of significant α-synuclein aggregation.

The age-related decline in cognitive ability of this model reflects a critical element of the development of symptoms seen in LBD patients. While the D409V/WT mouse does not show significant aggregates of α-synuclein in the hippocampus at 12 months, the presence of other pathological features of LBD support the hypothesis that this model at 12 months represents an early stage of LBD which is prime for effective therapeutic intervention which is translational to the clinic.

Historically, the Morris water maze has been used as a test of spatial learning and memory mediated predominantly by the hippocampus (Morris, 1984; Vorhees and Williams, 2006). In addition, it has been shown the Morris water maze involves the entorhinal and perirhinal cortices as well as involvement of the prefrontal cortex, the cingulate cortex and neostriatum, all areas implicated in LBD (Vorhees and Williams, 2006). Spontaneous alternation performance in the Y-maze, although controversial, is a measure of working memory also involving hippocampal circuits(Deacon and Rawlins, 2006). Accordingly, significant deficits in Morris water maze and Y-maze in D409V/WT mice at 12 months of age reported by this study implicate the hippocampus as a potential region of pathological interest. Pathological accumulation of α-synuclein and tau aggregates have been reported in the hippocampus of homozygous D409V/D409V *GBA1* mice at 6 months of age (Sardi, Clarke et al. 2011, 2013) suggesting that the hippocampus is particularly susceptible to significant reductions in GCase enzyme activity. Indeed, this study has showed that GCase enzyme activity in the hippocampus is far greater than seen in the cortex while Dopeso-Reyes et al. indicate that in non-human primate brain GCase protein is strongly expressed in the hippocampus (Dopeso-Reyes et al., 2018).

The lack of significant α-synuclein aggregates in the hippocampus of D409V/WT in this study may reflect a more subtle decline in GCase enzyme activity which is insufficient to result in accumulation of aggregates as seen in D409V/D409V mice (Sardi et al., 2011). However, despite failing to reach significance, perhaps a consequence of the low number of animals used for the experiment, there is a trend for increased soluble α-synuclein in the hippocampus of D409V/WT *GBA1* mice when compared to WT which is not seen in the cortex. However, these results should be interpreted with caution due to the limited number of animals particularly in the D409V/WT group. While sections were not pre-treated with proteinase K in order to unmask aggregates of α-synuclein as per Sardi et al. (Sardi et al., 2011), pre-treatment with proteinase K was tested with both D409V/WT and D409V/D409V hippocampal sections (data not shown) with no discernible staining of note. This finding was surprising since we were unable to replicate the

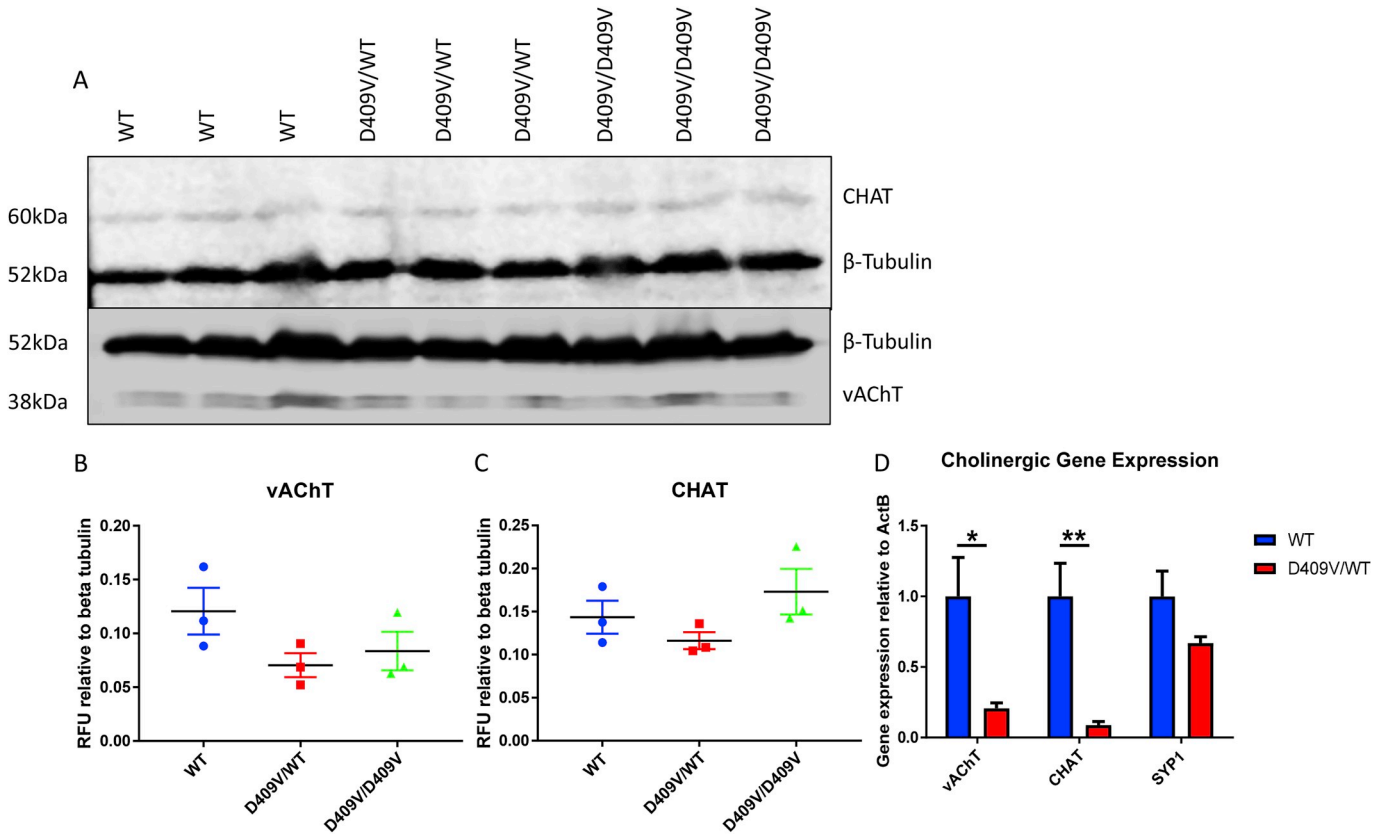

Fig. 7. Altered cholinergic protein and gene expression in the hippocampus of D409V mutant mice (a)representative western blots for vAChT, CHAT and β-Tubulin in the hippocampus of D409V mutant mice (b) Western blot quantification of vAChT. Data expressed as mean ± SEM. One way ANOVA $F(2,6) = 2.214$, $p = 0.190$, $n = 3$ mice per group. No significant difference between any genotype. (c) Western blot quantification of CHAT. Data expressed as mean ± SEM. One way ANOVA, $F(2,6) = 2.096$, $p = 0.2041$, $n = 3$ per group. No significant difference between any genotype. (d) Expression of *vAChT*, *CHAT* and *SYP1* mRNA relative to *ActB* as calculated using ΔΔct. Two-way ANOVA with Bonferroni correction, $F(1,18) = 24.77$, *$p = 0.0105$, **$p = 0.0034$, $n = 4$ mice per group.

α-synuclein staining profile in D409V/D409V hippocampus reported by Sardi et al. (Sardi et al., 2011).

It has been reported that in both human and mouse wild type/neurologically 'normal' brain, there is an age-related decline in GCase enzyme activity (Rocha et al., 2015a,b; Hallett et al., 2018). The presentation of cognitive impairment in D409V/WT mice at 12 months may reflect the additive impact of reduced GCase enzyme activity conferred by the presence of one mutant *GBA1* allele and the age related decline in GCase enzyme activity, providing a possible explanation why Sardi et al. did not see any cognitive impairment or obvious pathology in D409V/WT mice when tested at 6 months of age (Sardi et al., 2011). Furthermore, based upon this hypothesis, assessing α-synuclein accumulation in D409V/WT *GBA1* aged longer than 12 months may prove to uncover significant α-synuclein aggregates. Mice aged to between 18 and 24 months are considered to have human equivalence of 56–69 years, a more translational age for detection of the symptoms and the pathology associated with LBD (Dutta and Sengupta, 2016).

The significant reduction in activated *GBA1* derived GCase enzyme activity in the hippocampus D409V/WT mice in this study mirrors what has been previously reported in the literature. However, while an almost complete ablation of activated *GBA1* enzyme activity is seen in homozygous mice, the reduction in D409V/WT hippocampus reported in this study of approximately 71–72% is higher than the previously reported 41% at 6 months of age (Sardi et al., 2011). This finding provides further evidence for the additive impact of age-related decline in GCase enzyme activity.

Strikingly, *GBA2* derived GCase activity in the hippocampus and cortex of both WT and *GBA1* mutant mice is far greater than activated *GBA1* GCase enzyme activity. This finding suggests that *GBA2* derived GCase is the predominant GCase species in the brain. This observation is supported by a similar finding reported by Burke et al. (Burke et al., 2013). Glycosphingolipid metabolism is complex. While GluCer is the primary substrate for *GBA1* lysosomal GCase, it is also a substrate for an alternative pathway in which acid ceramidase can de-acylate glucosylceramide to glucosylsphingosine (GluSph) in the lysosome. Since GluSph has reduced hydrophobicity it is able to diffuse out of lysosomes into the cytoplasm where cytoplasmic *GBA2* GCase hydrolyses GluSph in to sphingosine and then sphingosine −1 – phosphate toxic metabolites. It has been reported that *GBA2* expression and *GBA2* derived GCase activity is increased in response to *GBA1* deficiency as a potential compensatory mechanism (Yildiz et al., 2006; Burke et al., 2013; Mistry et al., 2014). However, this compensatory increase in *GBA2* derived GCase activity may negatively impact cells via the increased sphingosine production from GluCer and GluSph (Massimo et al., 2016).

In this study, we report a highly significant reduction in *GBA2* GCase enzyme activity in the hippocampus of D409V/WT mice. The activity of *GBA2* GCase and accumulation of GluSph is of increasing interest in the field, with some suggesting the accumulation of GluSph precedes GluCer in Gaucher's disease(Dai et al., 2016; Taguchi et al., 2017). Not only does this hypothesis implicate reductions in both *GBA2* (causing accumulation of GluSph) and *GBA1* GCase enzyme activity (causing surplus GluCer which can be acetylated to GluSph) in LBD, both of which are reported in this study, it may explain why early studies did not find accumulation of GluCer in GBA-PD human brain (Gegg et al., 2015). Furthermore, it has been postulated that GluSph and not GluCer as previously thought (Mazzulli et al., 2011) promotes endogenous α-synuclein aggregation due to the templating propensity

of oligomeric α-synuclein species associated specifically with the presence of GluSph(Taguchi et al., 2017). In this context, our finding of significantly reduced *GBA2* GCase activity specifically in the hippocampus of D409V/WT mice is an important finding with implications for pathogenic mechanisms relating to accumulation and aggregation of α-synuclein which requires further investigation.

Cholinergic signalling from the medial septum and diagonal band of Broca to the hippocampus is critical for the formation of spatial memories (Ballinger et al., 2016). Indeed, it is known that an important role of the septal network is as a pacemaker for hippocampal rhythmic oscillations (Mamad et al., 2015). Loss of cholinergic neurons in the nucleus basalis of Meynert are strongly associated with Parkinson's disease, with many considering the cholinergic lesion associated with Parkinson's disease dementia to be greater than associated with Alzheimer's disease (Ballinger et al., 2016). Interestingly, patient's with PD dementia show a greater response to cholinesterase inhibitors than patients with AD. Unsurprisingly therefore, the functional integrity of forebrain cholinergic circuitry is essential for efficient performance of rodents in the Morris water maze. Water maze deficits have been reported in rats lesioned in the nucleus basalis of Meynert, medium septum and diagonal band of Broca (D'Hooge and De Deyn, 2001). In this study we were able to reflect altered cholinergic integrity associated with LBD. D409V/WT *GBA1* mice showed the most significant cholinergic changes in the hippocampus at 12 months of age. A highly significant reduction in staining for vAChT suggests that cholinergic neurons are unable to package acetylcholine into synaptic vesicles in preparation for release into the synaptic cleft and subsequently cholinergic neurotransmission within the hippocampus is impaired. An alternative explanation is that vAChT gene expression has been downregulated at the hippocampal synapse due to reduced cholinergic transmission. Increased staining for CHAT within the same neurons suggests a possible compensatory increase in the production of acetylcholine in response to the suggested impaired cholinergic neurotransmission. Further studies quantifying acetylcholine release in hippocampal synapses within these mice are required to confirm this hypothesis. Additionally, assessment of post synaptic hippocampal muscarinic and nicotinic acetylcholine receptors and electrophysiology to assess cholinergic transmission within the hippocampus would be beneficial.

Neuroinflammation is a common feature of many neurodegenerative diseases. Microglial activation in the substantial nigra in the absence of neurodegeneration has been reported in mice with *GBA1* deficiency in midbrain neurons (Soria et al., 2017). Furthermore, sustained inhibition of *GBA1* GCase enzyme activity in CβE treated mice causes significant microglial activation throughout the brain (Rocha et al., 2015a,b). Here, we were able to replicate characteristic microglial proliferation in the brain of D409V/WT mice, providing further evidence for the suitability of this model to study LBD. Additionally, we were able to demonstrate prominent astrogliosis within the hippocampus of D409V/WT mice. It has been suggested that a function of astrocytes in the hippocampus is as intermediaries of the septal cholinergic modulation of hippocampal neurons (Pabst et al., 2016). Astrogliosis in D409V/WT mice may therefore be further indication of cholinergic dysregulation.

It may be that the combination of cognitive impairment in the absence of significant α-synuclein aggregation in the hippocampus of D409V/WT *GBA1* mice reflects a 'pre-synuclein' early stage of LBD where cholinergic aberrations and glial accumulation are evident and predate Lewy body formation. This mouse model mirrors several aspects of LBD: age-related cognitive impairment implicating the hippocampus, cholinergic dysregulation, and evidence of accumulated astrocytes and microglia. The D409V/WT *GBA1* mouse may therefore be considered beneficial for the development of biomarkers and early therapeutic interventions for LBD.

Declarations of interest

None.

Funding

This work was supported by a grant from Alzheimer's Society, UK. We also acknowledge the Edmond J Safra Foundation for supporting this work by funding the maintenance of the GBA mouse colony. Chanati Jantrachotechatchawan was supported by the DPST PhD scholarship from the Thai government.

Appendix A. Supplementary data

Supplementary data to this article can be found online at https://doi.org/10.1016/j.neuint.2019.104502.

References

Ballinger, E.C., Ananth, M., Talmage, D.A., Role, L.W., 2016. Basal forebrain cholinergic circuits and signaling in cognition and cognitive decline. Neuron 91 (6), 1199–1218.
Beavan, M., McNeill, A., Proukakis, C., Hughes, D.A., Mehta, A., Schapira, A.H., 2015. Evolution of prodromal clinical markers of Parkinson disease in a GBA mutation-positive cohort. JAMA Neurol. 72 (2), 201–208.
Brockmann, K., Srulijes, K., Hauser, A.K., Schulte, C., Csoti, I., Gasser, T., Berg, D., 2011. GBA-associated PD presents with nonmotor characteristics. Neurology 77 (3), 276–280.
Burke, D.G., Rahim, A.A., Waddington, S.N., Karlsson, S., Enquist, I., Bhatia, K., Mehta, A., Vellodi, A., Heales, S., 2013. Increased glucocerebrosidase (GBA) 2 activity in GBA1 deficient mice brains and in Gaucher leucocytes. J. Inherit. Metab. Dis. 36 (5), 869–872.
Chahine, L.M., Qiang, J., Ashbridge, E., Minger, J., Yearout, D., Horn, S., Colcher, A., Hurtig, H.I., Lee, V.M., Van Deerlin, V.M., Leverenz, J.B., Siderowf, A.D., Trojanowski, J.Q., Zabetian, C.P., Chen-Plotkin, A., 2013. Clinical and biochemical differences in patients having Parkinson disease with vs without GBA mutations. JAMA Neurol. 70 (7), 852–858.
Chiasserini, D., Paciotti, S., Eusebi, P., Persichetti, E., Tasegian, A., Kurzawa-Akanbi, M., Chinnery, P.F., Morris, C.M., Calabresi, P., Parnetti, L., Beccari, T., 2015. Selective loss of glucocerebrosidase activity in sporadic Parkinson's disease and dementia with Lewy bodies. Mol. Neurodegener. 10, 15.
Clark, L.N., Chan, R., Cheng, R., Liu, X., Park, N., Parmalee, N., Kisselev, S., Cortes, E., Torres, P.A., Pastores, G.M., Vonsattel, J.P., Alcalay, R., Marder, K., Honig, L.L., Fahn, S., Mayeux, R., Shelanski, M., Di Paolo, G., Lee, J.H., 2015. Gene-wise association of variants in four lysosomal storage disorder genes in neuropathologically confirmed Lewy body disease. PLoS One 10 (5), e0125204.
D'Hooge, R., De Deyn, P.P., 2001. Applications of the Morris water maze in the study of learning and memory. Brain Res. Brain Res. Rev. 36 (1), 60–90.
Dai, M., Liou, B., Swope, B., Wang, X., Zhang, W., Inskeep, V., Grabowski, G.A., Sun, Y., Pan, D., 2016. Progression of behavioral and CNS deficits in a viable murine model of chronic neuronopathic gaucher disease. PLoS One 11 (9), e0162367.
Davis, M.Y., Johnson, C.O., Leverenz, J.B., Weintraub, D., Trojanowski, J.Q., Chen-Plotkin, A., Van Deerlin, V.M., Quinn, J.F., Chung, K.A., Peterson-Hiller, A.L., Rosenthal, L.S., Dawson, T.M., Albert, M.S., Goldman, J.G., Stebbins, G.T., Bernard, B., Wszolek, Z.K., Ross, O.A., Dickson, D.W., Eidelberg, D., Mattis, P.J., Niethammer, M., Yearout, D., Hu, S.C., Cholerton, B.A., Smith, M., Mata, I.F., Montine, T.J., Edwards, K.L., Zabetian, C.P., 2016 Oct 1. Association of GBA mutations and the E326K polymorphism with motor and cognitive progression in Parkinson disease. JAMA Neurol. 73 (10), 1217–1224.
Deacon, R.M., Rawlins, J.N., 2006. T-maze alternation in the rodent. Nat. Protoc. 1 (1), 7–12.
Dopeso-Reyes, I.G., Sucunza, D., Rico, A.J., Pignataro, D., Marin-Ramos, D., Roda, E., Rodriguez-Perez, A.I., Labandeira-Garcia, J.L., Lanciego, J.L., 2018. Glucocerebrosidase expression patterns in the non-human primate brain. Brain Struct. Funct. 223 (1), 343–355.
Dutta, S., Sengupta, P., 2016. Men and mice: relating their ages. Life Sci. 152, 244–248.
Fleming, S.M., Ekhator, O.R., Ghisays, V., 2013. Assessment of sensorimotor function in mouse models of Parkinson's disease. J. Vis. Exp. 76.
Gan-Or, Z., Giladi, N., Rozovski, U., Shifrin, C., Rosner, S., Gurevich, T., Bar-Shira, A., Orr-Urtreger, A., 2008. Genotype-phenotype correlations between GBA mutations and Parkinson disease risk and onset. Neurology 70 (24), 2277–2283.
Gegg, M.E., Burke, D., Heales, S.J., Cooper, J.M., Hardy, J., Wood, N.W., Schapira, A.H., 2012. Glucocerebrosidase deficiency in substantia nigra of Parkinson disease brains. Ann. Neurol. 72 (3), 455–463.
Gegg, M.E., Sweet, L., Wang, B.H., Shihabuddin, L.S., Sardi, S.P., Schapira, A.H., 2015. No evidence for substrate accumulation in Parkinson brains with GBA mutations. Mov. Disord. 30 (8), 1085–1089.
Ginns, E.I., Choudary, P.V., Tsuji, S., Martin, B., Stubblefield, B., Sawyer, J., Hozier, J., Barranger, J.A., 1985. Gene mapping and leader polypeptide sequence of human glucocerebrosidase: implications for Gaucher disease. Proc. Natl. Acad. Sci. U. S. A. 82 (20), 7101–7105.

Goker-Alpan, O., Giasson, B.I., Eblan, M.J., Nguyen, J., Hurtig, H.I., Lee, V.M., Trojanowski, J.Q., Sidransky, E., 2006. Glucocerebrosidase mutations are an important risk factor for Lewy body disorders. Neurology 67 (5), 908–910.
Goker-Alpan, O., Lopez, G., Vithayathil, J., Davis, J., Hallett, M., Sidransky, E., 2008. The spectrum of parkinsonian manifestations associated with glucocerebrosidase mutations. Arch. Neurol. 65 (10), 1353–1357.
Grabowski, G.A., 2008. Phenotype, diagnosis, and treatment of Gaucher's disease. Lancet 372 (9645), 1263–1271.
Guerreiro, R., Ross, O.A., Kun-Rodrigues, C., Hernandez, D.G., Orme, T., Eicher, J.D., Shepherd, C.E., Parkkinen, L., Darwent, L., Heckman, M.G., Scholz, S.W., Troncoso, J.C., Pletnikova, O., Ansorge, O., Clarimon, J., Lleo, A., Morenas-Rodriguez, E., Clark, L., Honig, L.S., Marder, K., Lemstra, A., Rogaeva, E., St George-Hyslop, P., Londos, E., Zetterberg, H., Barber, I., Braae, A., Brown, K., Morgan, K., Troakes, C., Al-Sarraj, S., Lashley, T., Holton, J., Compta, Y., Van Deerlin, V., Serrano, G.E., Beach, T.G., Lesage, S., Galasko, D., Masliah, E., Santana, I., Pastor, P., Diez-Fairen, M., Aguilar, M., Tienari, P.J., Myllykangas, L., Oinas, M., Revesz, T., Lees, A., Boeve, B.F., Petersen, R.C., Ferman, T.J., Escott-Price, V., Graff-Radford, N., Cairns, N.J., Morris, J.C., Pickering-Brown, S., Mann, D., Halliday, G.M., Hardy, J., Trojanowski, J.Q., Dickson, D.W., Singleton, A., Stone, D.J., Bras, J., 2018. Investigating the genetic architecture of dementia with Lewy bodies: a two-stage genome-wide association study. Lancet Neurol. 17 (1), 64–74.
Hall, H., Reyes, S., Landeck, N., Bye, C., Leanza, G., Double, K., Thompson, L., Halliday, G., Kirik, D., 2014. Hippocampal Lewy pathology and cholinergic dysfunction are associated with dementia in Parkinson's disease. Brain 137 (Pt 9), 2493–2508.
Hallett, P.J., Huebecker, M., Brekk, O.R., Moloney, E.B., Rocha, E.M., Priestman, D.A., Platt, F.M., Isacson, O., 2018. Glycosphingolipid levels and glucocerebrosidase activity are altered in normal aging of the mouse brain. Neurobiol. Aging 67, 189–200.
Hughes, R.N., 2004. The value of spontaneous alternation behavior (SAB) as a test of retention in pharmacological investigations of memory. Neurosci. Biobehav. Rev. 28 (5), 497–505.
Jellinger, K.A., 2018. Dementia with Lewy bodies and Parkinson's disease-dementia: current concepts and controversies. J. Neural Transm. 125 (4), 615–650 Vienna.
Jesus, S., Huertas, I., Bernal-Bernal, I., Bonilla-Toribio, M., Caceres-Redondo, M.T., Vargas-Gonzalez, L., Gomez-Llamas, M., Carrillo, F., Calderon, E., Carballo, M., Gomez-Garre, P., Mir, P., 2016. GBA variants influence motor and non-motor features of Parkinson's disease. PLoS One 11 (12), e0167749.
Kurzawa-Akanbi, M., Hanson, P.S., Blain, P.G., Lett, D.J., McKeith, I.G., Chinnery, P.F., Morris, C.M., 2012. Glucocerebrosidase mutations alter the endoplasmic reticulum and lysosomes in Lewy body disease. J. Neurochem. 123 (2), 298–309.
Livak, K.J., Schmittgen, T.D., 2001. Analysis of relative gene expression data using real-time quantitative PCR and the 2(-Delta Delta C(T)) Method. Methods 25 (4), 402–408.
Lunde, K.A., Chung, J., Dalen, I., Pedersen, K.F., Linder, J., Domellof, M.E., Elgh, E., Macleod, A.D., Tzoulis, C., Larsen, J.P., Tysnes, O.B., Forsgren, L., Counsell, C.E., Alves, G., Maple-Grodem, J., 2018. Association of glucocerebrosidase polymorphisms and mutations with dementia in incident Parkinson's disease. Alzheimers Dement 14 (10), 1293–1301.
Mamad, O., McNamara, H.M., Reilly, R.B., Tsanov, M., 2015. Medial septum regulates the hippocampal spatial representation. Front. Behav. Neurosci. 9, 166.
Massimo, A., Maura, S., Nicoletta, L., Giulia, M., Valentina, M., Elena, C., Alessandro, P., Rosaria, B., Sandro, S., 2016. Current and novel aspects on the non-lysosomal beta-glucosylceramidase GBA2. Neurochem. Res. 41 (1–2), 210–220.
Mazzulli, J.R., Xu, Y.H., Sun, Y., Knight, A.L., McLean, P.J., Caldwell, G.A., Sidransky, E., Grabowski, G.A., Krainc, D., 2011. Gaucher disease glucocerebrosidase and alpha-synuclein form a bidirectional pathogenic loop in synucleinopathies. Cell 146 (1), 37–52.
McNeill, A., Duran, R., Hughes, D.A., Mehta, A., Schapira, A.H., 2012. A clinical and family history study of Parkinson's disease in heterozygous glucocerebrosidase mutation carriers. J. Neurol. Neurosurg. Psychiatry 83 (8), 853–854.
Medhurst, A.D., Pangalos, M.N., 2003. Application of TaqMan RT-PCR for real-time semiquantitative analysis of gene expression in the striatum. Methods Mol. Med. 79, 229–241.
Mistry, P.K., Liu, J., Sun, L., Chuang, W.L., Yuen, T., Yang, R., Lu, P., Zhang, K., Li, J., Keutzer, J., Stachnik, A., Mennone, A., Boyer, J.L., Jain, D., Brady, R.O., New, M.I., Zaidi, M., 2014. Glucocerebrosidase 2 gene deletion rescues type 1 Gaucher disease. Proc. Natl. Acad. Sci. U. S. A. 111 (13), 4934–4939.
Moors, T.E., Paciotti, S., Ingrassia, A., Quadri, M., Breedveld, G., Tasegian, A., Chiasserini, D., Eusebi, P., Duran-Pacheco, G., Kremer, T., Calabresi, P., Bonifati, V., Parnetti, L., Beccari, T., van de Berg, W.D.J., 2019. Characterization of brain lysosomal activities in GBA-related and sporadic Parkinson's disease and dementia with Lewy bodies. Mol. Neurobiol. 56 (2), 1344–1355.
Morris, R., 1984. Developments of a water-maze procedure for studying spatial learning in the rat. J. Neurosci. Methods 11 (1), 47–60.
Murphy, K.E., Gysbers, A.M., Abbott, S.K., Tayebi, N., Kim, W.S., Sidransky, E., Cooper, A., Garner, B., Halliday, G.M., 2014. Reduced glucocerebrosidase is associated with increased alpha-synuclein in sporadic Parkinson's disease. Brain 137 (Pt 3), 834–848.
Nalls, M.A., Duran, R., Lopez, G., Kurzawa-Akanbi, M., McKeith, I.G., Chinnery, P.F., Morris, C.M., Theuns, J., Crosiers, D., Cras, P., Engelborghs, S., De Deyn, P.P., Van Broeckhoven, C., Mann, D.M., Snowden, J., Pickering-Brown, S., Halliwell, N., Davidson, Y., Gibbons, L., Harris, J., Sheerin, U.M., Bras, J., Hardy, J., Clark, L., Marder, K., Honig, L.S., Berg, D., Maetzler, W., Brockmann, K., Gasser, T., Novellino, F., Quattrone, A., Annesi, G., De Marco, E.V., Rogaeva, E., Masellis, M., Black, S.E., Bilbao, J.M., Foroud, T., Ghetti, B., Nichols, W.C., Pankratz, N., Halliday, G., Lesage, S., Klebe, S., Durr, A., Duyckaerts, C., Brice, A., Giasson, B.I., Trojanowski, J.Q., Hurtig, H.I., Tayebi, N., Landazabal, C., Knight, M.A., Keller, M., Singleton, A.B., Wolfsberg, T.G., Sidransky, E., 2013. A multicenter study of glucocerebrosidase mutations in dementia with Lewy bodies. JAMA Neurol. 70 (6), 727–735.
Neudorfer, O., Giladi, N., Elstein, D., Abrahamov, A., Turezkite, T., Aghai, E., Reches, A., Bembi, B., Zimran, A., 1996. Occurrence of Parkinson's syndrome in type I Gaucher disease. QJM 89 (9), 691–694.
Neumann, J., Bras, J., Deas, E., O'Sullivan, S.S., Parkkinen, L., Lachmann, R.H., Li, A., Holton, J., Guerreiro, R., Paudel, R., Segarane, B., Singleton, A., Lees, A., Hardy, J., Houlden, H., Revesz, T., Wood, N.W., 2009. Glucocerebrosidase mutations in clinical and pathologically proven Parkinson's disease. Brain 132 (Pt 7), 1783–1794.
Nichols, W.C., Pankratz, N., Marek, D.K., Pauciulo, M.W., Elsaesser, V.E., Halter, C.A., Rudolph, A., Wojcieszek, J., Pfeiffer, R.F., Foroud, T., Parkinson Study Group, P.I., 2009. Mutations in GBA are associated with familial Parkinson disease susceptibility and age at onset. Neurology 72 (4), 310–316.
Pabst, M., Braganza, O., Dannenberg, H., Hu, W., Pothmann, L., Rosen, J., Mody, I., van Loo, K., Deisseroth, K., Becker, A.J., Schoch, S., Beck, H., 2016. Astrocyte intermediaries of septal cholinergic modulation in the Hippocampus. Neuron 90 (4), 853–865.
Parkkinen, L., Neumann, J., O'Sullivan, S.S., Holton, J.L., Revesz, T., Hardy, J., Lees, A.J., 2011. Glucocerebrosidase mutations do not cause increased Lewy body pathology in Parkinson's disease. Mol. Genet. Metab. 103 (4), 410–412.
Rocha, E.M., Smith, G.A., Park, E., Cao, H., Brown, E., Hallett, P., Isacson, O., 2015a. Progressive decline of glucocerebrosidase in aging and Parkinson's disease. Ann. Clin. Transl. Neurol. 2 (4), 433–438.
Rocha, E.M., Smith, G.A., Park, E., Cao, H., Graham, A.R., Brown, E., McLean, J.R., Hayes, M.A., Beagan, J., Izen, S.C., Perez-Torres, E., Hallett, P.J., Isacson, O., 2015b. Sustained systemic glucocerebrosidase inhibition induces brain alpha-synuclein aggregation, microglia and complement C1q activation in mice. Antioxidants Redox Signal. 23 (6), 550–564.
Sardi, S.P., Clarke, J., Kinnecom, C., Tamsett, T.J., Li, L., Stanek, L.M., Passini, M.A., Grabowski, G.A., Schlossmacher, M.G., Sidman, R.L., Cheng, S.H., Shihabuddin, L.S., 2011. CNS expression of glucocerebrosidase corrects alpha-synuclein pathology and memory in a mouse model of Gaucher-related synucleinopathy. Proc. Natl. Acad. Sci. U. S. A. 108 (29), 12101–12106.
Sardi, S.P., Clarke, J., Viel, C., Chan, M., Tamsett, T.J., Treleaven, C.M., Bu, J., Sweet, L., Passini, M.A., Dodge, J.C., Yu, W.H., Sidman, R.L., Cheng, S.H., Shihabuddin, L.S., 2013. Augmenting CNS glucocerebrosidase activity as a therapeutic strategy for parkinsonism and other Gaucher-related synucleinopathies. Proc. Natl. Acad. Sci. U. S. A. 110 (9), 3537–3542.
Seibenhener, M.L., Wooten, M.C., 2015. Use of the Open Field Maze to measure locomotor and anxiety-like behavior in mice. J. Vis. Exp. 96, e52434.
Seto-Salvia, N., Pagonabarraga, J., Houlden, H., Pascual-Sedano, B., Dols-Icardo, O., Tucci, A., Paisan-Ruiz, C., Campolongo, A., Anton-Aguirre, S., Martin, I., Munoz, L., Bufill, E., Vilageliu, L., Grinberg, D., Cozar, M., Blesa, R., Lleo, A., Hardy, J., Kulisevsky, J., Clarimon, J., 2012. Glucocerebrosidase mutations confer a greater risk of dementia during Parkinson's disease course. Mov. Disord. 27 (3), 393–399.
Sidransky, E., Nalls, M.A., Aasly, J.O., Aharon-Peretz, J., Annesi, G., Barbosa, E.R., Bar-Shira, A., Berg, D., Bras, J., Brice, A., Chen, C.M., Clark, L.N., Condroyer, C., De Marco, E.V., Durr, A., Eblan, M.J., Fahn, S., Farrer, M.J., Fung, H.C., Gan-Or, Z., Gasser, T., Gershoni-Baruch, R., Giladi, N., Griffith, A., Gurevich, T., Januario, C., Kropp, P., Lang, A.E., Lee-Chen, G.J., Lesage, S., Marder, K., Mata, I.F., Mirelman, A., Mitsui, J., Mizuta, I., Nicoletti, G., Oliveira, C., Ottman, R., Orr-Urtreger, A., Pereira, L.V., Quattrone, A., Rogaeva, E., Rolfs, A., Rosenbaum, H., Rozenberg, R., Samii, A., Samaddar, T., Schulte, C., Sharma, M., Singleton, A., Spitz, M., Tan, E.K., Tayebi, N., Toda, T., Troiano, A.R., Tsuji, S., Wittstock, M., Wolfsberg, T.G., Wu, Y.R., Zabetian, C.P., Zhao, Y., Ziegler, S.G., 2009. Multicenter analysis of glucocerebrosidase mutations in Parkinson's disease. N. Engl. J. Med. 361 (17), 1651–1661.
Simitsi, A., Koros, C., Moraitou, M., Papagiannakis, N., Antonellou, R., Bozi, M., Angelopoulou, E., Stamelou, M., Michelakakis, H., Stefanis, L., 2018. Phenotypic characteristics in GBA-associated Parkinson's disease: a study in a Greek population. J. Parkinson's Dis. 8 (1), 101–105.
Soria, F.N., Engeln, M., Martinez-Vicente, M., Glangetas, C., Lopez-Gonzalez, M.J., Dovero, S., Dehay, B., Normand, E., Vila, M., Favereaux, A., Georges, F., Lo Bianco, C., Bezard, E., Fernagut, P.O., 2017. Glucocerebrosidase deficiency in dopaminergic neurons induces microglial activation without neurodegeneration. Hum. Mol. Genet. 26 (14), 2603–2615.
Taguchi, Y.V., Liu, J., Ruan, J., Pacheco, J., Zhang, X., Abbasi, J., Keutzer, J., Mistry, P.K., Chandra, S.S., 2017. Glucosylsphingosine promotes alpha-synuclein pathology in mutant GBA-associated Parkinson's disease. J. Neurosci. 37 (40), 9617–9631.
Vorhees, C.V., Williams, M.T., 2006. Morris water maze: procedures for assessing spatial and related forms of learning and memory. Nat. Protoc. 1 (2), 848–858.
Westbroek, W., Gustafson, A.M., Sidransky, E., 2011. Exploring the link between glucocerebrosidase mutations and parkinsonism. Trends Mol. Med. 17 (9), 485–493.
Winder-Rhodes, S.E., Evans, J.R., Ban, M., Mason, S.L., Williams-Gray, C.H., Foltynie, T., Duran, R., Mencacci, N.E., Sawcer, S.J., Barker, R.A., 2013. Glucocerebrosidase mutations influence the natural history of Parkinson's disease in a community-based incident cohort. Brain 136 (Pt 2), 392–399.
Yildiz, Y., Matern, H., Thompson, B., Allegood, J.C., Warren, R.L., Ramirez, D.M., Hammer, R.E., Hamra, F.K., Matern, S., Russell, D.W., 2006. Mutation of beta-glucosidase 2 causes glycolipid storage disease and impaired male fertility. J. Clin. Investig. 116 (11), 2985–2994.